STRUCTURAL CHEMISTRY

ISSN: 2053-2296
journals.iucr.org/c

$NaAl(SO_4)F_2$: a single-layer two-dimensional perovskite

Armel Le Bail, Lorentz Petter Lossius and Jone Finnestad

Acta Cryst. (2025). C**81**, 342–345

STRUCTURAL CHEMISTRY

ISSN 2053-2296

$NaAl(SO_4)F_2$: a single-layer two-dimensional perovskite

Armel Le Bail,[a]* Lorentz Petter Lossius[b] and Jone Finnestad[b]

[a]Le Mans Université, Institut des Molcules et des Matériaux du Mans, CNRS UMR 6283, Av. Olivier Messiaen, 72085 Le Mans, France, and [b]Hydro Aluminium AS, PO Box 303, NO-6882 Øvre Årdal, Norway. *Correspondence e-mail: armel.le_bail@univ-lemans.fr

Received 2 April 2025
Accepted 12 May 2025

Edited by I. Oswald, University of Strathclyde, United Kingdom

Keywords: fluorosulfate; perovskite; two-dimensional; powder diffraction; *ab initio*.

CCDC reference: 2450490

Supporting information: this article has supporting information at journals.iucr.org/c

The crystal structure of the sodium aluminium difluorosulfate $NaAl(SO_4)F_2$ has been determined from laboratory powder diffraction data. Its characterization allows for improving the monitoring of aluminium industrial production starting from cryolite. It is characterized by a perovskite single layer formed by the fluorine corner-sharing of $[AlF_4O_2]$ octahedra with SO_4 groups, and sodium as the interlayer content. This could be the $n = 1$ member of a possible new family of 2D perovskite materials $AM_n(SO_4)F_{3n-1}$ (A^+ = Na, Li; M^{3+} = Al, Fe, V, Cr), which remains to be confirmed.

1. Introduction

In 1997, the structure of $NaCaAlF_6$ was determined from powder diffraction data (Le Bail *et al.*, 1998), helping Hydro Aluminium to attain more accurate quantitative Rietveld analysis of frozen electrolyte baths from the Al-metal reduction cells. Since this previously not well-characterized phase was present in every bath sample, the result was important not only for Hydro Aluminium but the whole industry.

A new unknown phase occurred recently as a side-product during a test series with post-processing Al-metal cell bath electrolyte. This unknown was a major phase in some of the series reaction products requiring it to be structurally characterized to enable Rietveld quantitative phase analysis.

2. Experimental

2.1. Powder pattern measurement

The diffractometer used was a CubiX PRO built especially by PANalytical for primary aluminium-metal smelter operations, the bath acidity version, with long sharp focus and a single-point detector. It can only run up to 89° (2θ), as there is an XRF–Ca single channel at 90° (2θ). To moderate preferred orientation, the holder was backfilled and laid on a medium coarse filter paper. The sample was milled for a short time in a wolfram carbide lined ring and puck mill, so the average grain size was a relatively coarse 25 µm.

2.2. Structure solution and refinement

Using the indexing software *McMaille* (Le Bail, 2004), a tetragonal cell was proposed. A whole-pattern fitting without a structural model was made by the so-called Le Bail method (Le Bail, 2005) using the *FULLPROF* software (Rodríguez-Carvajal, 1993), confirming the unit cell and allowing the determination of the systematic extinctions leading to the space group $P4_2/ncm$ (see Fig. S1 in the supporting informa-

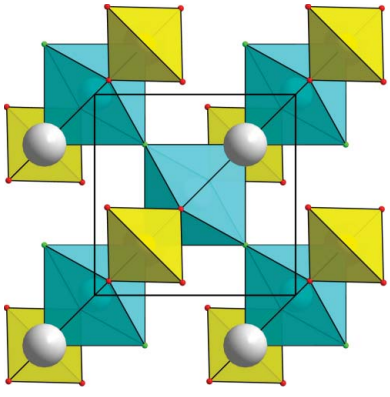

Table 1
Experimental details.

Crystal data	
Chemical formula	$NaAl(SO_4)F_2$
M_r	184.03
Crystal system, space group	Tetragonal, $P4_2/ncm$
Temperature (K)	293
a, c (Å)	4.9196 (3), 17.8704 (9)
V (Å)^3	432.51 (4)
Z	4
Radiation type	X-ray, Cu $K\alpha$
μ (mm^{-1})	9.75
Specimen shape, size (mm)	Plate, 15 × 15 × 1
Data collection	
Diffractometer	CubiX-PRO
Specimen mounting	Plate sample holder
Data collection mode	Reflection
Scan method	Step
2θ values (°)	$2\theta_{min}$ = 7.01, $2\theta_{max}$ = 87.99, $2\theta_{step}$ = 0.02
Refinement	
R factors and goodness-of-fit	R_p = 11.07, R_{wp} = 14.50, R_{exp} = 4.43, R_{Bragg} = 9.46, χ^2 = 10.69
No. of parameters	49

Computer programs: *McMaille* (Le Bail, 2004) for indexing, *FULLPROF* (Rodríguez-Carvajal, 1993) for intensity extraction and Rietveld refinement, *DIAMOND* (Brandenburg, 1999) for crystal structure drawing and *SHELXS97* (Sheldrick, 2008) for structure solution.

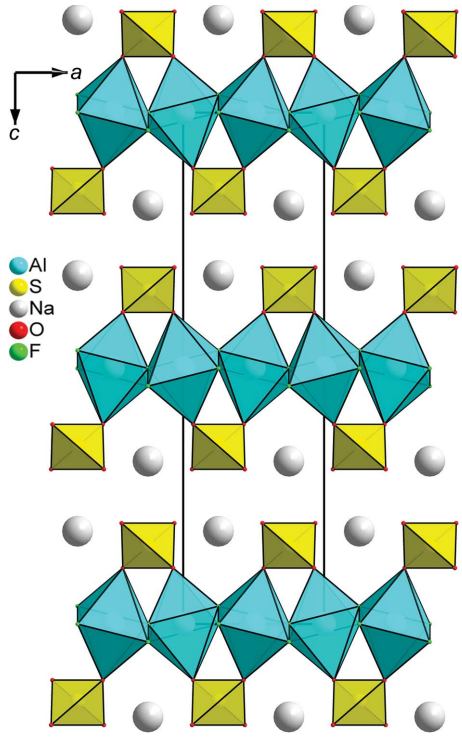

Figure 2
Unit-cell projection of the $NaAl(SO_4)F_2$ structure along the b axis, showing the $[AlF_4O_2]$ octahedra in blue forming perovskite-type planes by sharing their F corners. The SO_4 tetrahedra are in yellow and the Na atoms are in grey.

tion). From the previous fit, intensities were extracted (106 values) and used for structure solution. The direct methods implemented in the *SHELXS* software (Sheldrick, 2008) provided a complete model, with the S atom at the head. Since Na, Al, F and O have close scattering factors, they were undifferentiated at this stage (all designated by Q). But a close inspection of the interatomic distances allowed for a clear position attribution to Al, Na and O/F. In the powder pattern, after a few cycles of Rietveld refinement (Rietveld, 1969), still using the *FULLPROF* software, the presence of a preferred orientation along (001) was disclosed, which is not surprising given the 2D character of the structure (see below). Improvements were made by taking account of a main impurity (<5%) of $CaSO_4$ (Hawthorne & Ferguson, 1975) and traces (<1%) of β-AlF_3 (Le Bail *et al.*, 1988). It would certainly be better to have a powder pattern without preferred orientation and going to a larger maximum angle, but the current result, in spite of a high R_{Bragg} factor of 9.46% (R_F = 6.65%), attributed

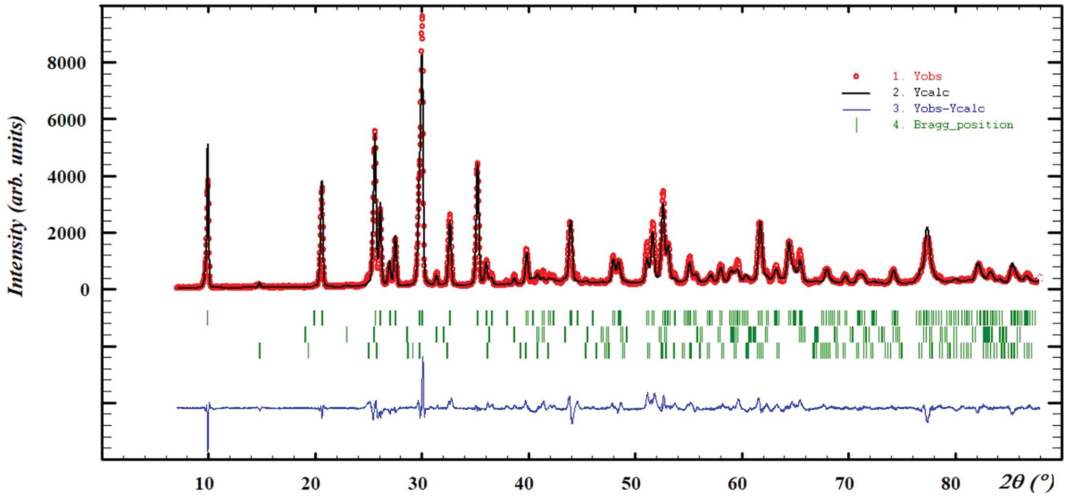

Figure 1
Rietveld fit from laboratory data for $NaAl(SO_4)F_2$. Red dots represent the observed data and the black line represents the calculated pattern. Bragg ticks are the peak positions (main phase at the top, then the two impurities, sulfate anhydrite $CaSO_4$ and β-AlF_3, at the bottom). The blue curve shows the difference between the observed and calculated patterns.

to the difficulty of taking account of this preferred orientation, looks acceptable for an industrial pattern optimized for speed (Fig. 1). Unfortunately, this exceptionally high concentrated sample is now used up. Crystal data, data collection and structure refinement details are summarized in Table 1.

3. Results and discussion

The $NaAl(SO_4)F_2$ formula is in accordance with the XRF estimation ($Na_{1.06}Al_{1.18}S_{0.99}O_{4.13}F_{2.27}Ca_{0.06}$), Ca being explained by the presence of $CaSO_4$. A projection of the structure along the *b* axis is shown on Fig. 2. $[AlF_4O_2]$ octahedra share their F corners to form a perovskite layer. The O corners of two adjacent octahedra are shared with one SO_4 group on both sides of the layer, causing one of the octahedra tilt systems noted $(\varphi 00)/(0\varphi 0)$, which occurs also in hybrid layered perovskites with the $n = 1$ Ruddlesden–Popper structure belonging to the same space group (Liu *et al.*, 2023). The tilts run about axes along $[1\bar{1}0]$ in the first layer and [110] in the second layer (Figs. 3 and 4). The Na^+ cations are in a pentagonal bipyramid (NaO_6F), completing the interlayer content (Fig. 5). A bond valence analysis (see Table 2 in the supporting information) reports values close to the expected values.

Only one compound was found to have a similar formula, $SrFe(PO_4)F_2$ (Le Meins *et al.*, 1997). However, its structure consists of chains of (FeO_2F_4) and (FeO_4F_2) octahedra sharing corners and interlinked by PO_4 tetrahedra so as to form a 2D framework between which the Sr^{2+} cations are inserted. The $[FePO_4F_2]$ sheet is topologically identical to the structural unit of the mineral Laueite (Moore, 1965).

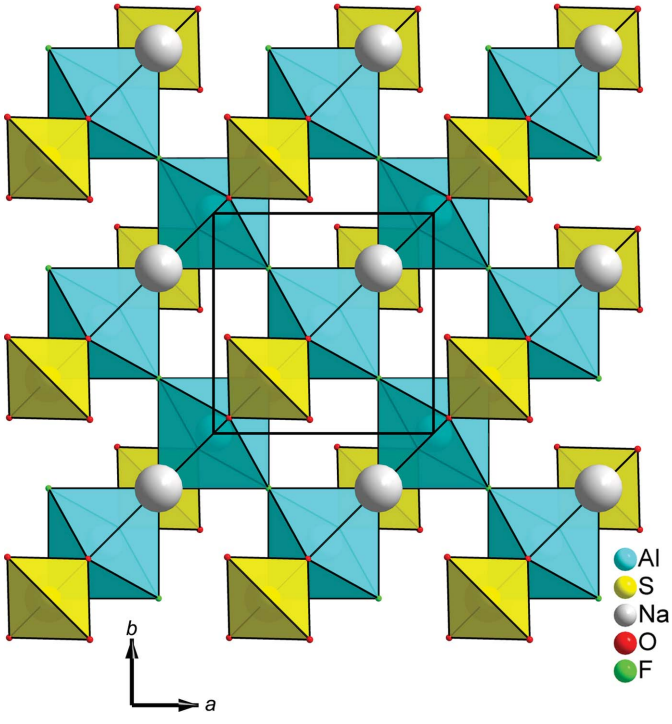

Figure 3
The perovskite layer at $z = 0$. Octahedra rotate along axes in the $[1\bar{1}0]$ direction.

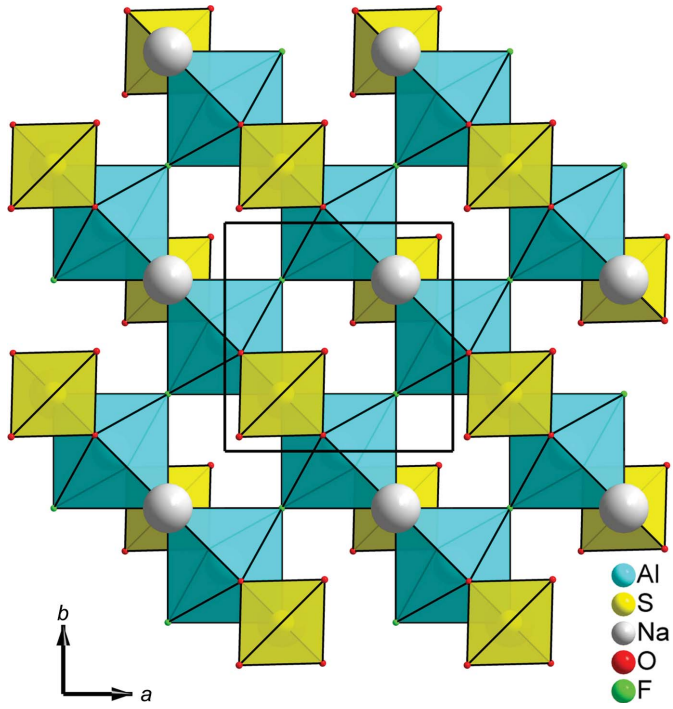

Figure 4
The perovskite layer at $z = \frac{1}{2}$. Octahedra rotate along axes in the [110] direction.

Alkali metal fluorosulfates (and fluorophosphates) adopt a rich variety of compositions and structures. Those with the $AMBO_4F$ formulation (A = Li, Na; M = Fe, Co, Ni, *etc.*; B = P, S) have applications for high-voltage electrode materials (Barpanda & Tarascon, 2013). Their structures are essentially built from chains of corner-sharing octahedra or from bi-octahedral units made by face-sharing. $NaAl(SO_4)F_2$ is the first fluorosulfate example of a layered perovskite ($n = 1$) and so belongs to those quasi-2D perovskites having many applications in industry. It becomes a candidate on the route for the emerging perovskite monolayers (Ricciardulli *et al.*, 2021). Imagining bilayers (or more, $n > 1$) with analogous interlayer content is easy but remains to be realized in order to have a new family of 2D perovskite materials, $AM_n(SO_4)F_{3n-1}$ (A^+ =

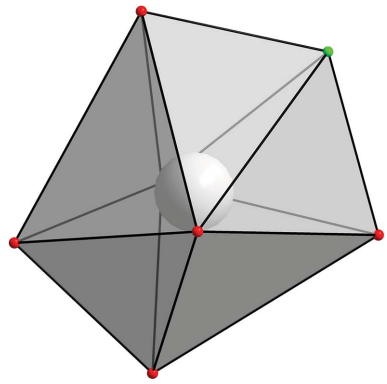

Figure 5
Seven-coordinated sodium $[NaO_6F]$ in a pentagonal-based bipyramid.

Na, Li; M^{3+} = Al, Fe, V, Cr), to be added to those Ruddlesden–Popper, Dion–Jacobson and Aurivillius well-known materials, or those where organic molecules separate inorganic sheets (Smith *et al.*, 2018). Work on this is in progress.

4. Related literature

The following references are cited in the supporting information for this article: Brese & O'Keeffe (1991); Brown & Altermatt (1985).

Acknowledgements

Thanks are expressed to Fluorsid and the team at Hydro TOS Laboratory Porsgrunn, and especially Erik Tveten and Jakob Løyning for the synthesis and isolation, and to Hydro Aluminium Metal, Alcoa, Fluorsid and SINTEF for allowing us to publish this article. The project is co-sponsored by the Research Council of Norway.

Funding information

Funding for this research was provided by: Norges Forskningsrd (grant No. 317798).

References

Barpanda, P. & Tarascon, J.-M. (2013). *Lithium Batteries: Advanced Technologies and Applications*, edited by B. Scrosati, K. M. Abraham, W. A. van Schalkwijk & J. Hassoun, ch. 7, pp. 127–160. New York: John Wiley & Sons Inc.

Brandenburg, K. (1999). *DIAMOND*. Crystal Impact GbR, Bonn, Germany.

Brese, N. E. & O'Keeffe, M. (1991). *Acta Cryst.* B**47**, 192–197.

Brown, I. D. & Altermatt, D. (1985). *Acta Cryst.* B**41**, 244–247.

Hawthorne, F. C. & Ferguson, R. B. (1975). *Can. Mineral.* **13**, 289–292.

Le Bail, A. (2004). *Powder Diffr.* **19**, 249–254.

Le Bail, A. (2005). *Powder Diffr.* **20**, 316–326.

Le Bail, A., Hemon-Ribaud, A. & Courbion, G. (1998). *Eur. J. Solid State Inorg. Chem.* **35**, 265–272.

Le Bail, A., Jacoboni, C., Leblanc, M., De Pape, R., Duroy, H. & Fourquet, J. L. (1988). *J. Solid State Chem.* **77**, 96–101.

Le Meins, J.-M., Hemon-Ribaud, A., Laligant, Y. & Courbion, G. (1997). *Eur. J. Solid State Inorg. Chem.* **34**, 391–404.

Liu, T., Holzapfel, N. P. & Woodward, P. M. (2023). *IUCrJ*, **10**, 385–396.

Moore, P. B. (1965). *Am. Mineral.* **50**, 1884–1892.

Ricciardulli, A. G., Yang, S., Smet, J. H. & Saliba, M. (2021). *Nat. Mater.* **20**, 1325–1336.

Rietveld, H. M. (1969). *J. Appl. Cryst.* **2**, 65–71.

Rodríguez-Carvajal, J. (1993). *Physica B*, **192**, 55–69.

Sheldrick, G. M. (2008). *Acta Cryst.* A**64**, 112–122.

Smith, M. D., Crace, E. J., Jaffe, A. & Karunadasa, H. I. (2018). *Annu. Rev. Mater. Res.* **48**, 111–136.

supporting information

Acta Cryst. (2025). C**81**, 342-345 [https://doi.org/10.1107/S2053229625004280]

$NaAl(SO_4)F_2$: a single-layer two-dimensional perovskite

Armel Le Bail, Lorentz Petter Lossius and Jone Finnestad

Computing details

(I)

Crystal data

$AlF_2O_4S·(Na)$
M_r = 184.03
Tetragonal, $P4_2/ncm$
Hall symbol: -P 4ac 2ac
a = 4.9196 (3) Å
c = 17.8704 (9) Å
V = 432.51 (4) Å^3
Z = 4
$F(000)$ = 360
D_x = 2.826 Mg m^{-3}
Cu $K\alpha$ radiation, λ = 1.540560 Å
T = 293 K
Particle morphology: powder of platelets
white
Specimen preparation: Prepared at 293 K

Data collection

CubiX-PRO diffractometer
Radiation source: X-ray
Specimen mounting: plate sample holder
Data collection mode: reflection
Scan method: step
$2\theta_{min}$ = 7.044°, $2\theta_{max}$ = 88.024°, $2\theta_{step}$ = 0.020°

Refinement

R_p = 11.066
R_{wp} = 14.498
R_{exp} = 4.435
R_{Bragg} = 9.46
4050 data points
Profile function: pseudo-Voigt
49 parameters
0 restraints
Background function: manual
Preferred orientation correction: (001) direction, p=0.803(3)

Fractional atomic coordinates and isotropic or equivalent isotropic displacement parameters (Å^2)

	x	y	z	U_{iso}*/U_{eq}
Na	0.25000	0.25000	0.8166 (2)	0.0013 (14)*
Al	0.00000	0.50000	0.50000	0.0095 (13)*
S	0.25000	0.25000	0.65070 (17)	0.0044 (9)*
O1	0.0703 (7)	0.4297 (7)	0.6090 (3)	0.0127 (13)*
O2	0.0607 (8)	0.0607 (8)	0.6946 (3)	0.0127 (13)*
F1	0.25000	0.25000	0.4663 (3)	0.0265 (17)*
F2	0.25000	0.75000	0.50000	0.0265 (17)*

Geometric parameters (Å, º)

Al—O1	2.008 (6)	Na—O2^{iii}	2.547 (6)
Al—O1^{i}	2.008 (6)	Na—O2^{vi}	2.171 (4)
Al—F1	1.8406 (18)	Na—O2^{vii}	2.171 (4)
Al—F1^{i}	1.8406 (18)	Na—F1^{viii}	2.675 (7)
Al—F2	1.7393	O1—O1^{iii}	2.500 (5)
Al—F2^{ii}	1.7393	O1—O2	2.374 (7)
S—O1	1.455 (5)	O1—F1	2.840 (7)
S—O1^{iii}	1.455 (5)	O1—F1^{i}	2.603 (5)
S—O2	1.533 (5)	O1—F2	2.657 (5)
S—O2^{iii}	1.533 (5)	O1—F2^{ii}	2.657 (5)
Na—O1^{iv}	2.595 (5)	O2—O2^{iii}	2.634 (6)
Na—O1^{v}	2.595 (5)	F1—F2^{ix}	2.5324 (13)
Na—O2	2.547 (6)		
O1—Al—O1^{i}	180.0 (5)	O1^{iv}—Na—O2	89.7 (3)
O1—Al—F1	95.0 (4)	O1^{iv}—Na—O2^{iii}	152.0 (4)
O1—Al—F1^{i}	85.0 (3)	O1^{iv}—Na—O2^{vi}	92.7 (3)
O1—Al—F2	90.0 (3)	O1^{iv}—Na—O2^{vii}	92.7 (3)
O1—Al—F2^{ii}	90.0 (3)	O1^{iv}—Na—F1^{viii}	59.2 (2)
O1^{i}—Al—F1	85.0 (3)	O1^{v}—Na—O2	152.0 (4)
O1^{i}—Al—F1^{i}	95.0 (4)	O1^{v}—Na—O2^{iii}	89.7 (3)
O1^{i}—Al—F2	90.0 (3)	O1^{v}—Na—O2^{vi}	92.7 (3)
O1^{i}—Al—F2^{ii}	90.0 (3)	O1^{v}—Na—O2^{vii}	92.7 (3)
F1—Al—F1^{i}	180.00 (18)	O1^{v}—Na—F1^{viii}	59.2 (2)
F1—Al—F2	90.00 (8)	O2—Na—O2^{iii}	62.3 (3)
F1—Al—F2^{ii}	90.00 (8)	O2—Na—O2^{vi}	85.5 (3)
F1^{i}—Al—F2	90.00 (8)	O2—Na—O2^{vii}	85.5 (3)
F1^{i}—Al—F2^{ii}	90.00 (8)	O2—Na—F1^{viii}	148.9 (4)
F2—Al—F2^{ii}	180.000	O2^{iii}—Na—O2^{vi}	85.5 (3)
O1—S—O2^{iii}	105.2 (5)	O2^{iii}—Na—O2^{vii}	85.5 (3)
O1^{iii}—S—O2	105.2 (5)	O2^{iii}—Na—F1^{viii}	148.9 (4)
O1^{iii}—S—O2^{iii}	105.2 (5)	O2^{vi}—Na—O2^{vii}	169.4 (4)
O2—S—O2^{iii}	118.4 (5)	O2^{vi}—Na—F1^{viii}	95.3 (3)
O1^{iv}—Na—O1^{v}	118.4 (3)	O2^{vii}—Na—F1^{viii}	95.3 (3)

Symmetry codes: (i) −*x*, −*y*+1, −*z*+1; (ii) *y*−1, *x*, *z*; (iii) −*x*+1/2, −*y*+1/2, *z*; (iv) *y*−1/2, −*x*, −*z*+3/2; (v) −*y*+1, *x*+1/2, −*z*+3/2; (vi) *y*+1/2, −*x*, −*z*+3/2; (vii) −*y*, *x*+1/2, −*z*+3/2; (viii) −*y*+1/2, *x*, *z*+1/2; (ix) *x*, *y*−1, *z*.

*Valence bond analysis according to the empirical expression from Brown & Altermatt (1985), using parameters for solids from Brese & O'Keeffe (1991). References: Brese, N. E. & O'Keefe, M. (1991). Acta Cryst. B**47**, 192–197; Brown, I. D. & Altermatt, D. (1985). Acta Cryst. B**41**, 244–247.*

	O1	O2	F1	F2	Σ	Σexpected
Na	0.118	0.370x2 0.134x2	0.067		1.31	2
Al	0.350x2		0.450x2 x2	0.591x2 x2	2.78	3

S	1.575x2	1.279x2			5.71	6
Σ	2.04	1.78	0.97	1.18		
Σexpected	2	2	1	1		